

Feature Enhancement of Retinal Images in Deep Convolution Pipeline, Its Reconstruction, Extraction and Analytical Evaluation

Mahua Nandy Pal

CSE Department

MCKV Institute of Engineering, MAKAUT, Kolkata, India

mahua.nandy@gmail.com

Minakshi Banerjee

CSE Department

RCC Institute of Information Technology, Kolkata, India

mbanerjee23@gmail.com

Abstract—Purpose: Retinal image analysis and segmentation gives us information regarding different ocular and cardio-vascular diseases. Retinal image enhancement is the important pre-requisite of retinal image analysis and segmentation. In recent era, deep network has been extensively used in different research fields. In this paper, we attempt to exploit the application of deep convolution in retinal image enhancement and evaluate it against traditional enhancement techniques which are most prevalently used for retinal image enhancement.

Method: We have utilized successive convolution and transposed convolution to enhance features of a retinal image. Feature maps are reconstructed from deep convolution layers and enhanced image is extracted successfully. We have evaluated the quality of the extracted enhanced image, with respect to three traditional enhancement techniques as well as different combinations of them. These traditional techniques are applications of contrast limited adaptive histogram equalization (CLAHE), adaptive gamma correction (AGC) and Tophat transformation. We evaluated all the methods on the basis of image quality assessment (IQA) metrics. Both statistical error based IQA metrics and visual information based IQA metrics are evaluated for this purpose. The metrics are peak signal to noise ratio (PSNR) and absolute mean brightness error (AMBE).

Results: Deep convolution enhanced retinal images are reconstructed and extracted successfully and compared with other enhancement schemes. In most of the experiments deep convolution based enhancement performs the best among all schemes in terms of both types of IQA metrics.

Conclusion: Deep convolution based enhancement can be used prior to retinal image segmentation and analysis instead of single or different arbitrary combinations of more than one single enhancement schemes for better precision in the relevant fields.

Keywords - Deep convolution; Transposed convolution; Feature map; PSNR; AMBE;

I. INTRODUCTION

Retinal image segmentation leads to the analysis of symptomatic manifestations of different ocular and circulatory diseases such as hypertension, diabetes, cardio vascular diseases etc. which are visible at an early stage in retinal fundus images. Challenges present in automated retinal image segmentation are presence of noise, low contrast, uneven illumination, minute sizes of medically significant local artifacts such as micro aneurysms, hemorrhages etc. In the process of automated image segmentation and analysis, image enhancement plays a vital role.

II. LITERATURE SURVEY

Adaptive histogram equalization (AHE) is an image contrast enhancement method. But it is time consuming and it suffers from excessive enhancement of insignificant features. These two problems are addressed by Pizer et al. in [1]. To take care of these two problems K. Zuiderveld in [2] proposed Contrast Limited Adaptive Histogram Equalization (CLAHE). CLAHE based retinal image pre processing method has been used in [3]. [4] contributed considerably in the field of image enhancement with AGC. They presented a transformation technique to improve brightness of the image through gamma correction and probability distribution of luminance pixels. [5] discussed application of AGC for different types of image enhancement. An image contrast based adaptive gamma

correction is present in [6]. A morphological transformation based enhancement method for medical images has been presented in [7]. [8] used different morphological operators and clustering for vessel segmentation. An entropy based image quality metric is discussed in [9]. [10] presented a comparative study of different pre processing techniques to enhance mammograms. [11] presented a survey on different retinal vessel segmentation algorithms. [12] iteratively thresholded the residual retinal image to obtain higher vessel segmentation accuracy. [13], [14] and [15] exploited deep learning architecture to identify vessels from retinal fundus images. Deep feature representations of retinal images has been utilized for content based retrieval of diabetic retinopathy (DR) image using Siamese CNN by Chung et al. [22]. A review on deep learning based retinal image analysis has been presented by Maryam Badar in [23].

[16] proposed U-net convolutional neural network model which is efficient in segmenting bio medical images. [26] is the application of U-Net on medical images. [27] presents a medical image enhancement application.

The contribution of the work is reconstruction and extraction of enhanced version of retinal image from deep convolution pipeline and to compare it quantitatively with other traditional image enhancement policies with application to retinal image analysis and segmentation. For deep convolution enhancement, U-type convolution pipeline has been implemented. Deep convolution enhancement has been compared with some enhancement techniques frequently used with retinal image analysis like - contrast limited adaptive histogram equalization, adaptive gamma correction and tophat transformation and their different combinations. Proper algorithms are given for enhanced image reconstruction and extraction from deep convolution pipeline. Our work quantitatively concludes that in most of the evaluation experiments, deep convolution enhancement performs better than other methods

III. DEEP CONVOLUTION IMAGE ENHANCEMENT

Deep convolution based image enhancement takes place following three consecutive sub phases. They are deep convolution, feature map reconstruction and enhanced image extraction. The network architecture and the three sub phases are described as follows.

A. Network Architecture

In our network, convolution layers have been implemented for image enhancement. We exploited U-type [16] convolution-deconvolution connections as it utilizes the same feature maps for contraction of the image to capture local artefacts of the image and for expansion of the vector to a reconstructed image by proper localization and placement of those artefacts. Thus semantic features are enhanced while structural integrity of image data is retained.

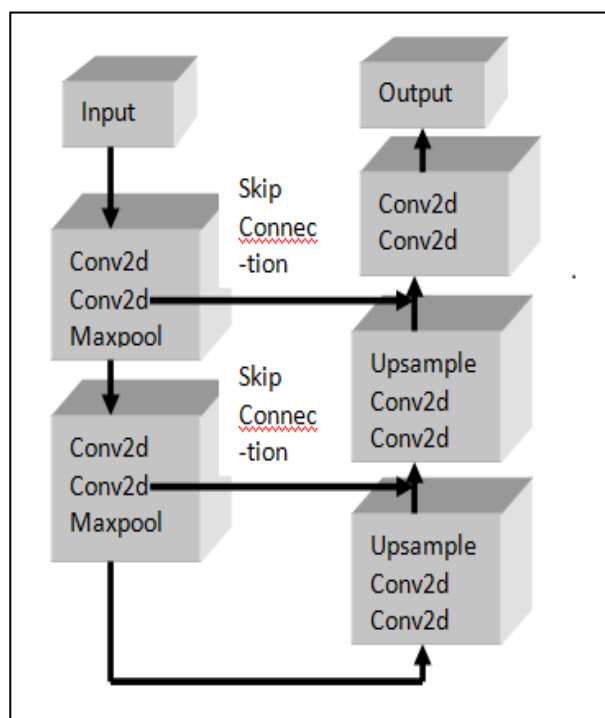


Figure 1. Enhancement network block diagram

In this deep convolution network, consecutive convolution and maxpooling layers of filter size 2x2 form the unit of contraction pathway and level wise consecutive transposed convolution and up sampling layers form the unit of expansion pathway. For better reconstruction at every step of expansion, skip connections are implemented to concatenate convolution and transposed convolution output. We implemented connections with two levels in contraction pathway and two levels in expansion pathway. A drop out of 0.2 has been employed between two consecutive convolution layers. ReLU is used as activation function with each of the convolution and transposed convolution layers. The block diagram for the enhancement network is as in figure 1.

B. Image Enhancement

Deep convolution network has multiple convolution layers and each of the layers produces a weight matrix or tensor. Feature maps of higher convolution level are spatially coarser but semantically stronger. This feature map information can be used to represent enhanced image. We enhance image with multiple number of convolutions.

The network is fed with a number of overlapping green channel image patches of size 48 x 48 and with a stride value of 20. If the image was fed to network as a whole it might be possible that minute local artefacts of retinal images remained unobserved in many cases. These green patches pass through convolution and transposed convolution layer following the network architecture as discussed in the previous subsection.

C. Feature Map Reconstruction

n number of overlapping patches of a fundus image with strides in height and width respectively are input to the model and model output size is $m * \text{patch_height} * \text{patch_width}$ where m is number of filters.

Overlapping image patches with stride values of 20 are considered for successful reconstruction of feature maps from patches without any grid line at the patch boundary. These patches pass through both contraction and expansion pathway. We extracted patch feature maps of shape 48x48 from the final layer of transposed convolution stack in the expansion pathway. The feature map reconstruction algorithm is as follows,

Algorithm :FeatureMapReconstruction

Input Data:

1. `Img_height` = height of reconstructed map
2. `Img_width` = width of reconstructed map
3. `Stride_height` = stride in height at which patches are extracted
4. `Stride_width` = stride in width at which patches are extracted
5. `Patchset` = 3-D array of shape $[n, \text{patch_height}, \text{patch_width}]$

Intermediate Data:

1. `FullSum2D[Img_height,Img_width]`, initialized with all zeros
2. `TemporaryConstructedMap[Img_height, Img_width]`, initialized with all zeros

Output Data:

1. `FinalReconstructedMap`

begin

Set `Patch_height` = `patch_height`

Set `Patch_width` = `patch_width`

Set `N_patches_height` = $((\text{Img_height} - \text{Patch_height}) / \text{stride_height}) + 1$

Set `N_patches_width` = $((\text{Img_width} - \text{Patch_width}) / \text{stride_width}) + 1$

`Total_patches` = `N_patches_height` * `N_patches_width`

`k` = 0

for `h` in 1 to `N_patches_height` **do**

for `w` in 1 to `N_patches_width` **do**

`from_height` = $h * \text{stride_height}$,

`to_height` = $(h * \text{stride_height}) + \text{Patch_height}$

`from_width` = $w * \text{stride_width}$,

`to_width` = $(w * \text{stride_width}) + \text{Patch_width}$

`TemporaryConstructedMap[from_height:to_height,from_width: to_width]` + = `Patchset[k]`

`FullSum2D [from_height: to_height, from_width: to_width]` + = 1

`k` = `k`+1

end

end

FinalReconstructedMap = TemporaryConstructedMap / FullSum2D(element wise)

Return FinalReconstructedMap

end

D. Enhanced Image Extraction

We considered a pre defined number of maximum entropy patches to extract the enhanced image as per our experimental observations. High entropy feature maps at a particular level are merged together by element wise summation to produce a semantically stronger feature map which actually represents enhanced image in the convolution pipeline. The algorithm for enhanced image extraction from multiple feature maps is as follows,

Algorithm: EnhancedImageExtraction

Input Data:

1. Img_height = height of reconstructed map
2. Img_width = width of reconstructed map
3. Stride_height = stride in height at which patches are extracted
4. Stride_width = stride in width at which patches are extracted
5. FeatureMaps = 4-D array of shape [m, n, patch_height, patch_width]

Intermediate Data:

1. SingleChannelReconstructed[Img_height,Img_width], initialized with all zeros
2. FullSum2D[Img_height,Img_width], initialized with all zeros

Output Data:

1. EnhancedImage

Functions used:

1. Information_content(img): responsible for generating information content of an image “img” and returns its value as +1 if information content is more than required information threshold else return -1.

begin

Set Patch_height = patch_height

Set Patch_width = patch_width

k = 0

for i in 1 to m **do**

SingleChannelReconstructed = FeatureMapReconstruction(FeatureMaps[i], Img_height, Img_width, Stride_height, Stride_width)

If Information_content(SingleChannelReconstructed) > 0:

FullSum2D += SingleChannelReconstructed

end

end

EnhancedImage = FullSum2D

Return EnhancedImage

end

IV. IMPLEMENTATION SPECIFICATION

The system has been implemented using Intel Core i5-6500CPU @ 3.20 GHz, 6M Cache, upto 3.6 Ghz, 12 GB DDR4 RAM and NVIDIA GeForce GTX 1660 SUPERGPU with 1408 CUDA cores and 6GB of GDDR6 memory. Software specification for the work is as follows, Python 3.8.6 with NVIDIA CUDA 10.1. Different required side loaded modules are Tensorflow 2.3.1, Keras 2.4.3 etc.

V. ENHANCEMENT EVALUATION METRICS

We used two different categories of image quality assessment (IQA) metrics to evaluate effective enhancement policy. They are statistical error based metrics and human visual perception based metrics. In reality, most reliable IQA metric is provided by human observer who is responsible for making use of that image data to draw some inference. But this is the subjective way of IQA. Human perception is better represented by Human visual perception based metric. However, we considered both of them to evaluate our enhancement schemes. Peak signal to noise ratio (PSNR) is most prevalently used statistical error based IQA metric whereas absolute mean brightness error (AMBE) is the commonly used visual perception based IQA metric.

A. Peak Signal To Noise Ratio – PSNR

PSNR indicates the deviation of the enhanced image and the original image corresponding to the peak gray level value and is given by the equation 1.

$$\text{PSNR} = 10 \log \frac{(I_{\max})^2}{\text{MSE}} \quad (1)$$

MSE is mean squared error between the original image(I) and the enhanced image(En) and is given by equation 2.

$$\text{MSE} = \frac{1}{MN} \sum_{m,n} (\text{En}(m, n) - \text{I}(m, n))^2 \quad (2)$$

Higher value of PSNR indicates better information content of the enhanced image.

B. Absolute Mean Brightness Error- AMBE

AMBE is the absolute difference between expectations of enhanced and original images.

$$\text{AMBE} = |\text{E}(\text{En}) - \text{E}(\text{I})| \quad (3)$$

where E(En) and E(I) are expectations of original and enhanced images respectively. Lower the value of AMBE, lower is the contrast representation error of the enhanced image.

VI. DATASET DESCRIPTION

A. DRIVE

For experimental evaluation, DRIVE [20] retinal image dataset is used as it is the most used dataset among researchers. Each image was preserved with 8 bits per color plane and at resolution of 565 by 584 pixels. Among forty photographs, 33 are healthy and 7 show symptoms of mild early DR.

B. STARE

STARE [24] dataset is composed of 20 color images of retina. The image size is 700 x 605 pixels; 8 bits per color channel and are available in Portable Pixmap (.ppm) format. We evaluated 8 pathology samples separately to infer that the evaluation decision is equally applicable to affected images with varied ailments also.

C. Messidor

1200 eye fundus color images in Messidor database [25]. Images were stored with 8 bits per color plane and with 1440*960, 2240*1488 or 2304*1536 pixels. Total 12 subsets contain 100 images in TIFF format each and an excel file with medical diagnoses for each image. Two diagnoses have been, one is DR grade and another is risk of macular edema (ME).

VII. EXPERIMENTAL RESULTS

During enhancement, green channel of retinal image is only considered [9].

A. Deep Convolution Based enhancement

We considered image enhancement within deep convolution pipeline and evaluated image enhancement after 10th convolution as discussed previously. The entire feature maps of a particular image from 10th convolution layer have been shown in figure 2. The single enhanced image obtained from 10th convolution layer by merging high entropy feature maps with element wise summation. This enhanced image and its histogram are shown in figure 3.

B. Traditional Enhancement

We considered three different traditional enhancement techniques which are used most frequently for retinal image enhancement by the researchers. These are applications of CLAHE, AGC and Tophat transformation. We tested not only with these three single enhancement procedures, but also different combinations of them as used in the relevant literatures (figure 4). These evaluation results are compared with deep convolution based enhancement evaluation results.

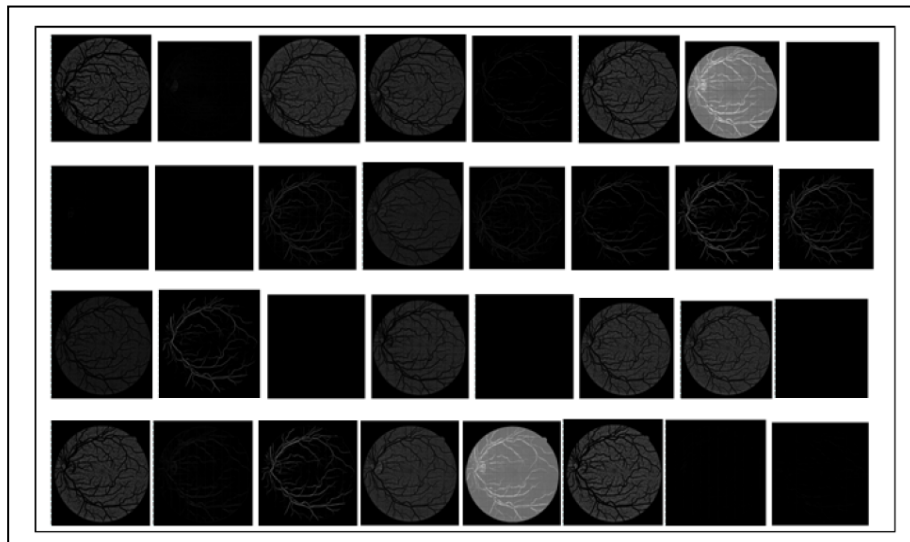


Figure 2. 32 feature maps at 10th deep convolution layer

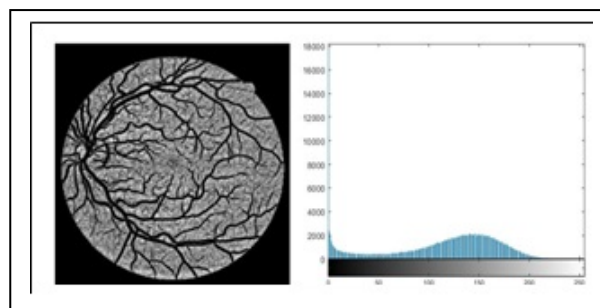


Figure 3. Deep 10th convolution enhanced image and its stretched histogram

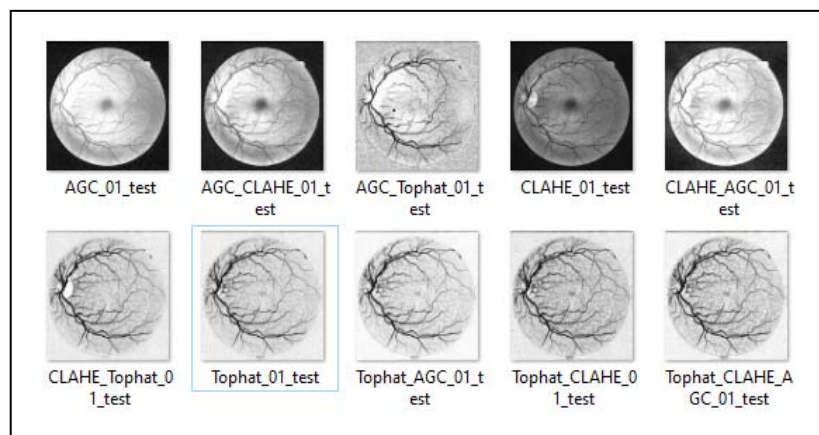


Figure 4. Different combinations of traditional enhancement methods

C. IQA Metric Based Enhancement Evaluation

Table I and II respectively display average values of PSNR and AMBE calculated over all the images of DRIVE dataset [20] and STARE dataset [24]. It has been found from most of the observations that deep convolution enhancement is the efficient alternative as compared to different traditional schemes.

TABLE I. AVERAGE PSNR VALUES FOR DRIVE AND STARE

Enhancement Techniques	Av. PSNR - DRIVE	Av. PSNR – STARE
CLAHE	21.3989	13.72
AGC	9.1297	11.2704
Tophat	4.2996	5.4768
AGC-Tophat	5.1962	5.3723
AGC-CLAHE	10.1491	12.3419
Tophat-AGC	3.8204	4.8698
Tophat-CLAHE	4.8734	6.5073
CLAHE-Tophat	4.4936	5.8972
CLAHE-AGC	8.0453	9.0230
Tophat-CLAHE_AG	4.3214	5.6954
Deep Convolution	15.6705	14.1053

TABLE II. AVERAGE AMBE VALUES FOR DRIVE AND STARE

Enhancement Techniques	Av. PSNR - DRIVE	Av. PSNR – STARE
CLAHE	16.4864	45.3766
AGC	76.3101	58.9972
Tophat	135.8085	116.7737
AGC-Tophat	123.3155	120.0581
AGC-CLAHE	68.2909	54.0020
Tophat-AGC	144.7504	126.7884
Tophat-CLAHE	119.3541	94.4954
CLAHE-Tophat	131.0733	107.7733
CLAHE-AGC	90.2071	81.6047
Tophat-CLAHE_AG	139.7946	107.6374
Deep Convolution	14.1673	22.2588

D. Effectiveness of deep convolution enhancement for identifying abnormalities

4 DRIVE test image samples, 10 Messidor Base 11 samples and 5 STARE images have been chosen for verifying the applicability of the general observation obtained in the previous sub section for affected images also. These chosen DRIVE samples are mild DR samples, Messidor samples are severely affected grade 3 DR along with grade 2 ME samples and STARE samples are having varied abnormality symptoms other than DR as available in the dataset information. Table III and IV show the average IQA performance measurements on those pathology samples separately to assess the effectiveness of deep convolution based image enhancement.

TABLE III. AVERAGE PSNR VALUES FOR DIFFERENT DATASET PATHOLOGY SAMPLES

Enhancement Techniques	Av. PSNR – DRIVE (Mild DR)	Av PSNR – Messidor (Severe DR & ME)	Av. PSNR – STARE (Varied Abnormality Symptoms)
CLAHE	24.3606	13.9827	14.7294
AGC	9.9341	6.6335	11.6027
Tophat	4.6716	2.6151	5.5359
AGC-Tophat	5.5559	5.0871	5.4776
AGC-CLAHE	11.1675	7.7958	12.9225
Tophat-AGC	4.1596	2.1593	4.9547
Tophat-CLAHE	5.2340	2.9332	6.5194
CLAHE-Tophat	4.9289	2.8158	6.0095
CLAHE-AGC	8.8479	5.6311	9.4742
Tophat-CLAHE_AGC	4.6517	2.4579	5.7440
Deep Convolution	14.8634	20.9529	13.2132

TABLE IV. AVERAGE AMBE VALUES FOR DIFFERENT DATASET PATHOLOGY SAMPLES

Enhancement Techniques	Av. AMBE – DRIVE (Mild DR)	Av. AMBE – Messidor (Severe DR & ME)	Av. AMBE – STARE (Varied Abnormality Symptoms)
CLAHE	30.5249	32.0906	36.7220
AGC	70.0331	90.2734	56.8877
Tophat	127.0265	171.2960	113.1700
AGC-Tophat	115.9515	112.9789	116.8927
AGC-CLAHE	62.2053	78.6206	49.9511
Tophat-AGC	136.4187	180.8022	122.7804
Tophat-CLAHE	111.4148	162.1828	90.7236
CLAHE-Tophat	121.2600	165.6620	102.4505
CLAHE-AGC	83.8836	101.9464	75.9353
Tophat_CLAHE_AGC	122.2841	171.9283	103.5098
Deep Convolution	24.9537	8.3741	25.4895

E. Graphical Observation of Enhancement Evaluation

Average IQA metric values for DRIVE and STARE databases and the same for variably affected images from three different databases have been represented graphically from figure 5 to 8.

VIII. DISCUSSION

Different ailment symptoms are evident in retina at a very early phase. Image enhancement is the pre-requisite of image segmentation and analysis.

We constructed an image enhancement deep convolution network following the concept of feature map reconstruction after a series of convolution feature enhancement steps. We considered reconstruction of feature maps and extraction of enhanced image from deep convolution pipe line. Detailed algorithms for both feature map reconstruction and enhanced image extraction from deep convolution pipeline are given in a separate subsection.

To quantify enhancement quality both statistically and visually we considered PSNR and AMBE as the representatives of both types of IQA metrics respectively. Higher PSNR value and lower AMBE value indicate better quality of enhanced image. Considering both categories of IQA metrics enhancement performance achieved by different enhancement methods are as observed in table 3 and 4. Figures 5 and 6 provide proper visualization of average IQA performance on DRIVE and STARE dataset images respectively.

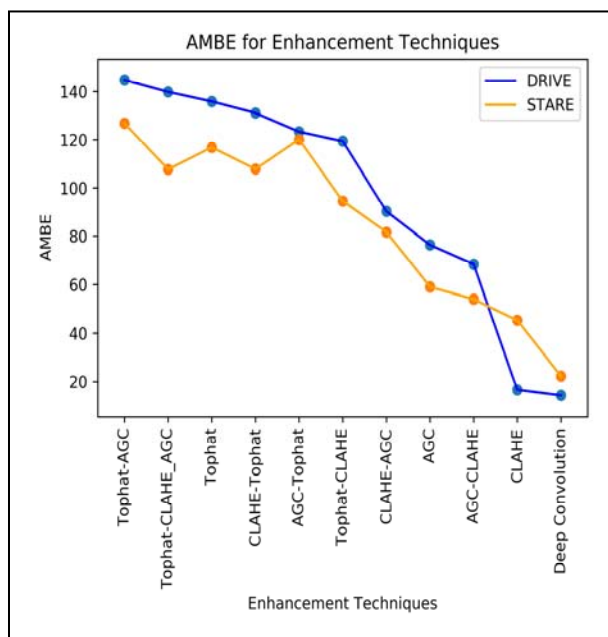


Figure 5. Average AMBE values of DRIVE and STARE for different enhancement schemes

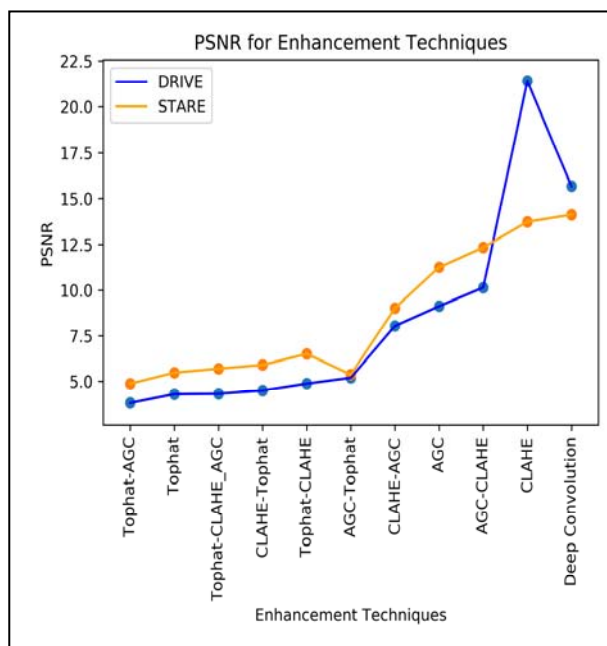


Figure 6. Average PSNR values of DRIVE and STARE for different enhancement schemes

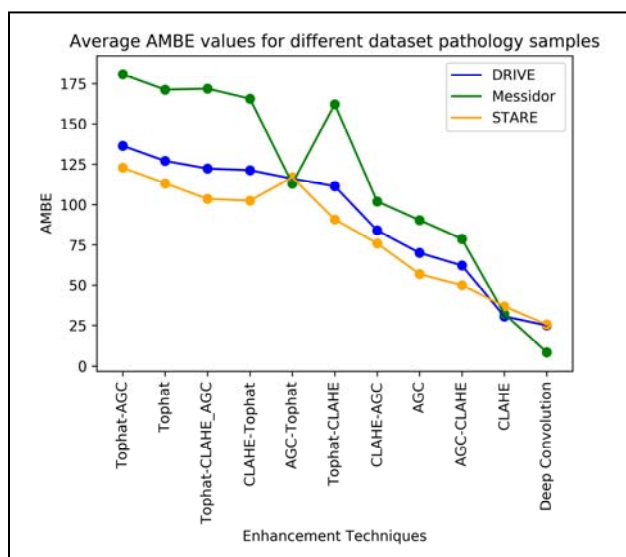


Figure 7. Average AMBE evaluation for varied ailment symptoms using DRIVE, STARE and Messidor Base 11 pathology samples

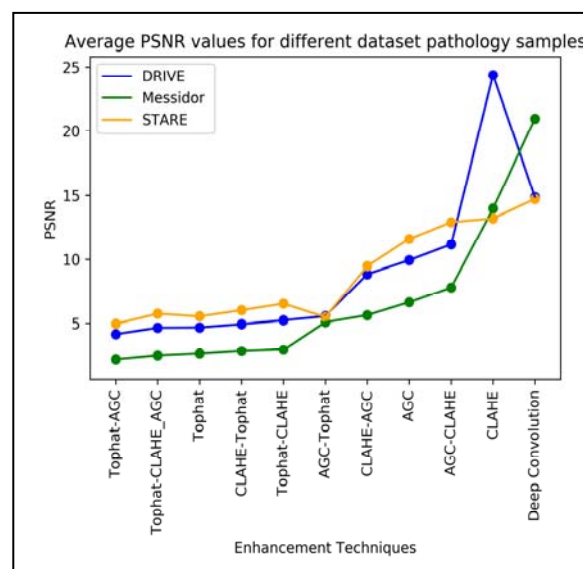


Figure 8. Average PSNR evaluation for varied ailment symptoms using DRIVE, STARE and Messidor Base 11 pathology samples

Effectiveness of deep convolution enhancement has been assessed particularly for abnormal retinal fundus images and the obtained results have been discussed in a separate sub section. For abnormal image evaluation mild DR samples from DRIVE test set, severe DR and severe ME samples from Messidor base 11 dataset and a wide variety of abnormal (other than DR) images from STARE dataset have been selected. Table 5 and 6 represent average values of different IQA performance metrics computed on abnormal DRIVE, STARE and Messidor dataset images respectively. The graphical visualization of the same has been available in figures 7 and 8.

Thus, considering overall performances over both types of IQA evaluation, it may be stated that deep convolution enhancement performance is good enough for image enhancement when applied to varied datasets. But one thing is noticeable in our observations that CLAHE enhanced DRIVE samples show high value of average PSNR for whole dataset evaluation as well as abnormal test images evaluation. This is the observational exception applicable to a particular dataset only. Though other two concerned dataset results help us to conclude steadily that deep convolution enhancement is the best option among the different alternatives. Sometimes

statistical error based metrics may not represent visual perception properly. Hence, we may rely more on visual perception based metrics while drawing inference about better image enhancement. According to AMBE, deep convolution enhancement is the most effective one considering diverse datasets with diverse disease symptoms.

To ascertain our observational discussion, we represent some deep convolution enhanced abnormal images from DRIVE dataset with mild DR symptoms in figure 9 for better visual perception of effective image enhancement. The observational exceptions regarding average PSNR values of DRIVE images may be due to the existence of minute mild DR symptoms which are missed out during enhancement.

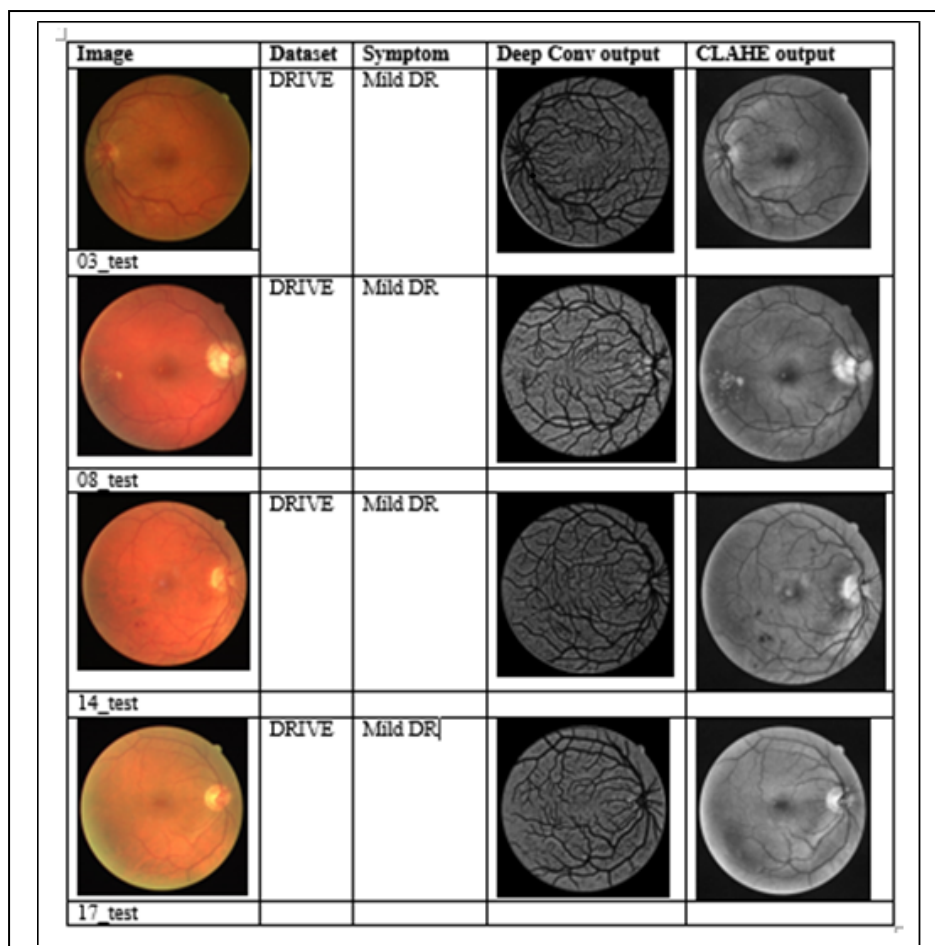


Figure 9. Visual perception of DRIVE mild DR samples using deep convolution and CLAHE

IX. CONCLUSION

In this paper, we utilized deep convolution network for retinal image enhancement. We reconstructed feature maps and extracted enhanced images from deep convolution pipeline.

We evaluated these output images with other traditional enhancement technique outputs. On the basis of our majority observations, it is quantitatively evaluated that deep convolution enhancement performs best among all of them while applied for retinal image segmentation and analysis.

REFERENCES

- [1] Pizer, S., Amburn, E., Austin, J., Cromartie, R., Geselowitz, A., Greer, T., terHaarRomeny, B., Zimmerman, J., and Zuiderveld, K. Adaptive histogram equalization and its variations. *Computer Vision, Graphics and Image Processing*, 39, pp. 355-368, 1987.
- [2] Zuiderveld, K. Contrast limited adaptive histogram equalization. Chapter VIII.5, *Graphics Gems, IV*, pp. 474-485, 1994.
- [3] Nandy Pal, M. and Banerjee, M., A Comparative Analysis of Application of Niblack and Sauvola Binarization to Retinal Vessel Segmentation. In *proc. CINE 2017, IEEE Xplore*.
- [4] Huang, S., Cheng, F., and Chiu, Y. Efficient contrast enhancement using adaptive gamma correction with weighting distribution. *IEEE Transaction on Image Processing*, 22, 2013.
- [5] Rahman, S., Rahman, M., Abdullah-Al-Wadud, M., Al-Quaderi, G., and Shoyaib, M. An adaptive gamma correction for image enhancement. *Eurasip Journal on Image and Video Processing*, 35, 2016.
- [6] Nandy, M. and Banerjee, M. Automatic diagnosis of micro aneurysm manifested retinal images by deep learning method. In *Proceedings, ICETST 2019*.
- [7] Hassanpour, H., Samadiani, N., and Mahdi Salehi S.M. Using morphological transforms to enhance the contrast of medical images. *The Egyptian Journal of Radiology and Nuclear Medicine*, 46, pp. 481-489, 2015.

- [8] Hassan, G., El-Bendary, N., Hassanien, A., Fahmy, A., Shoeb, A., and Snasel, V. Retinal blood vessel segmentation approach based on mathematical morphology. *Procedia Computer Science*, 65, 612-622, 2015.
- [9] Nandy, M. and Banerjee, M. Retinal vessel segmentation using gabor filter and artificial neural network. In *Proceedings, IEEE International Conference on Emerging Applications of Information Technology - EAIT 2012*, pp. 157-160, 2012.
- [10] Sheba, K. and Gladston, R. Objective quality assessment of image enhancement methods in digital mammography-a comparative study. *Signal and Image Processing : An International Journal*, 7, 2016.
- [11] Almotiri, J., Elleithy, K., and Elleithy, A. Retinal vessels segmentation techniques and algorithms: A survey. *Applied Sciences*, 8, 2018.
- [12] Roychowdhury, S., Koozekanani, D., and Parhi, K. K. Iterative vessel segmentation of fundus images. *IEEE Transactions on Biomedical Engineering*, 62, pp. 1738-1749, 2015.
- [13] Fu, H., Xu, Y., Lin, S., Wong, D., and Liu, J. Deep vessel: Retinal vessel segmentation via deep learning and conditional random field. In *proceedings, Medical Image Computing and Computer Assisted Intervention MICCAI 2016*, pp. 132-139. 2016.
- [14] Liskowski, P. and Krawiec, K. (2016) Segmenting retinal blood vessels with deep neural networks. *IEEE Transactions on Medical Imaging*, 35, pp. 2369- 2380, 2016.
- [15] Mo, J. and Zhang, L., Multi-level deep supervised networks for retinal vessel segmentation. *International Journal of Computer Assisted Radiology and Surgery*, 12, 21812193, December, 2017.
- [16] Ronneberger, O., Fischer, P., and Brox, T. U-net:convolutional networks for biomedical image segmentation. *arXiv:1505.04597v1 [cs.CV]* 18 May 2015.
- [17] Cai, J., Gu, S., and Zhang, L. Learning a deep single image contrast enhancer from multi-exposer images. *IEEE Transactions on Image Processing*, 27, pp. 2049-2062, 2018.
- [18] Singh, S. and Bovis, K., An evaluation of contrast enhancement techniques for mammographic breast masses. *Chapter VIII.5, Graphics Gems IV.*, 9, pp. 109-119, 2005.
- [19] Staal, J., Abrano, A., Niemeijer, M., Viergever, M., and Ginneken, B., Ridge based vessel segmentation in color images of the retina. *IEEE Transactions on Medical Imaging*, 23, pp. 501-509, 2004.
- [20] Digital retinal image for vessel extraction (DRIVE). Image Sciences Institute, Link: <http://www.isi.uu.nl/Research/Databases/DRIVE/>, online accessed on 25/06/2020.
- [21] Gonzalez, R. C. and Woods, R. E. *Digital Image Processing*. 3rd Edition, Pearson.
- [22] Yu An Chung, Wei Hung Weng, "Learning Deep Representations of Medical Images using Siamese CNNs with Application to Content based Image Retrieval", In *Proc. 31st Conf, on Neural Information Processing Systems, NIPS 2017, USA, Dec. 2017*.
- [23] MayamBadar, Muhammad Haris, Anam Fatima, "Application of Deep Learning for Retinal Image Analysis: A Review", *Computer Science Review, Elsevier*, 35, 100203, 2020.
- [24] Structured Analysis of the Retina (STARE). Clemson University, <https://cecas.clemson.edu/~ahoover/stare/>, online, accessed 1-July-2018.
- [25] MESSIDOR Dataset, A consortium of Universities and Laboratories, Link: <http://www.adcis.net/en/third-party/messidor/>, online accessed on 25/06/2020.
- [26] Oskal, K. R., Risdal, M., Janssen, E. A., Undersrud, E. S., & Gulsrud, T. O., A U-net based approach to epidermal tissue segmentation in whole slide histopathological images. *SN Applied Sciences*, 1(7), 672. 2019.
- [27] Reddy, G. B., & Kumar, H. P., Enhancement of mammogram images by using entropy improvement approach. *SN Applied Sciences*, 1(12), 1688, 2019.